



Responses of the Coral Symbiont *Cladocopium goreaui* to Extreme Temperature Stress in Relatively High-Latitude Reefs, South China Sea

Lifei Wei¹ · Shuchang Chen¹ · Zhenjun Qin¹ · Nengbin Pan¹ · Mengling Lan¹ · Tingchao Zhang¹ · Ran He¹ · Hongye Liang¹ · Wenzhi Deng¹ · Changhao Mo¹ · Kefu Yu^{1,2}

Received: 10 April 2025 / Accepted: 25 July 2025

© The Author(s) 2025

Abstract

Global climate change has led to frequent extreme temperature events in oceans. Corals are susceptible to extreme high-temperature stress in summer and extreme low-temperature stress in winter in the relatively high-latitude reef areas of the South China Sea (SCS). The most abundant symbiotic coral Symbiodiniaceae in the higher-latitude reefs of the SCS is *Cladocopium goreaui*, predominantly associating with dominant coral hosts such as *Acropora* and *Porites*. However, to date, relatively few studies have focused on the response and mechanism of *C. goreaui* to the extreme high- and low-temperature stress. In this study, the responses and regulatory mechanisms of the dominant *C. goreaui* to extreme high- and low-temperature stress were investigated based on physiological indexes, transmission electron microscopy (TEM), and transcriptome analysis. The results showed that (1) under 34 °C heat stress, the disintegration of thylakoids triggered photosynthetic collapse in *C. goreaui*; survival is enabled through metabolic reprogramming that upregulates five protective pathways and redirects energy via pentose/glucuronate shunting to sustain ATP homeostasis, revealing a trade-off between damage containment and precision energy governance under thermal extremes. (2) Low temperature exposure induced suppression of maximum quantum yield (F_v/F_m), compounded by glutathione pathway inhibition, crippling ROS scavenging. The transcriptome results revealed that *C. goreaui* prioritizes gene fidelity maintenance under low temperature stress. These findings reveal that energy allocation trade-offs constitute the core strategy of *C. goreaui* temperature response: prioritizing energy maintenance under high-temperature stress, while safeguarding genetic fidelity at the expense of antioxidant defense under low-temperature stress.

Keyword *Cladocopium goreaui* · Extreme high and low temperature · F_v/F_m ; Transcriptome

Introduction

The coral holobiont comprises the coral host, symbiotic microalgae (Symbiodiniaceae), and a diverse microbiota including bacteria, archaea, fungi, and viruses, which collectively drive nutrient cycling and stress resilience [1]. One of the most important symbiotic relationships is that between

the coral host and Symbiodiniaceae, which is a family of symbiotic dinoflagellates that form mutualistic associations with corals and other marine invertebrates [2]. However, this symbiotic partnership is highly vulnerable to environmental stressors, particularly temperature fluctuations that trigger coral bleaching—a phenomenon now imperiling the survival of coral reefs worldwide [3, 4].

Thermal sensitivity varies markedly among Symbiodiniaceae [2]. The *Cladocopium* genus is particularly sensitive to even moderate temperature increases. Such increases disrupt the structure of Photosystem II (PSII) and chloroplast-like vesicle membranes [5]. These changes limit CO₂ fixation and affect Symbiodiniaceae growth [6]. Under thermal stress, excessive production of reactive oxygen species (ROS) in chloroplasts leads to DNA, protein, and lipid damage [7]. ROS further impairs photosynthetic activity by inhibiting PSII repair mechanisms and disrupting photosynthetic membranes [6]. Excessive ROS

✉ Zhenjun Qin
qzj_gxu@163.com

✉ Kefu Yu
kefuyu@scsio.ac.cn

¹ Guangxi Laboratory On the Study of Coral Reefs in the South China Sea, Coral Reef Research Center of China, School of Marine Sciences, Guangxi University, Nanning 530004, China

² Southern Marine Science and Engineering Guangdong Laboratory (Guangzhou), Guangzhou, China

can cause coral tissue damage and discharge of symbiotic Symbiodiniaceae, leading to coral bleaching and death [8, 9]. In contrast to the extensively studied thermal stress, cold stress as another potential threat remains significantly under-researched. Sudden low temperatures caused by regional extreme low-temperature events such as oceanic cold currents can lead to extensive coral bleaching, death, and coral reef degradation [10]. Under marine cold-spells, Symbiodiniaceae exhibit cold-induced photoinhibition through impaired PSII function, characterized by decline in maximal photosynthetic efficiency, which triggers ROS accumulation and subsequent photodamage to thylakoid membranes. This results in the accumulation of ROS in tissues, coral bleaching, and death [8, 11, 12]. In the context of global warming, coral reefs at higher latitudes are gaining ecological prominence as potential climate refugia due to their cooler waters, which may offer thermal respite for sensitive coral species [13, 14]. However, their role as refugia is complicated by winter low-temperature stress, which itself poses a significant physiological challenge to coral survival [15].

High-latitude coral reefs occur in temperate regions and are characterized by seasonal temperature fluctuations and lower mean temperatures compared to tropical reefs [14]. High-latitude coral reefs are distributed worldwide, including locations such as Western Australia, South Africa, and Japan [14, 16, 17]. The South China Sea (SCS), with a relatively high latitude, belongs to the relatively high-latitude reef region. Relatively high-latitude coral reef areas in the SCS include the Weizhou Island (Guangxi), Daya Bay (Guangdong), Hong Kong, Dongshan (Fujian), and Taiwan [18–20]. The SST of the Weizhou Island (WI) waters can be as high as 32 °C at extremely high temperatures and as low as 12.3 °C at extremely low temperatures [21, 22]. In summer, marine heatwaves cause corals to undergo thermal bleaching in these regions. Meanwhile, marine cold-spells may cause cold bleaching in winter. Although Symbiodiniaceae heat responses are well-studied, their autonomous cold acclimation mechanisms in high-latitude SCS reefs remain elusive, with most research focusing on holobiont level responses [23–26]. *Cladocopium* dominates the Symbiodiniaceae community composition in SCS high-latitude coral reefs, with its prevalence exhibiting a positive latitudinal gradient correlated with seasonal temperature variability [27]. The mechanisms of how *C. goreau* responds to extremely high and low temperatures remain unclear.

This study systematically investigates *C. goreau*'s extreme temperature responses (34 °C heat stress/14 °C cold stress vs 26 °C control) using three complementary approaches: (1) F_v/F_m as a biomarker for photosystem impairment; (2) transmission electron microscopy (TEM) revealing ultrastructural changes; and (3) transcriptomics identifying DEGs in energy metabolism, protein folding,

and stress signaling. These collectively address how high-latitude populations reconfigure gene networks to withstand thermal fluctuations.

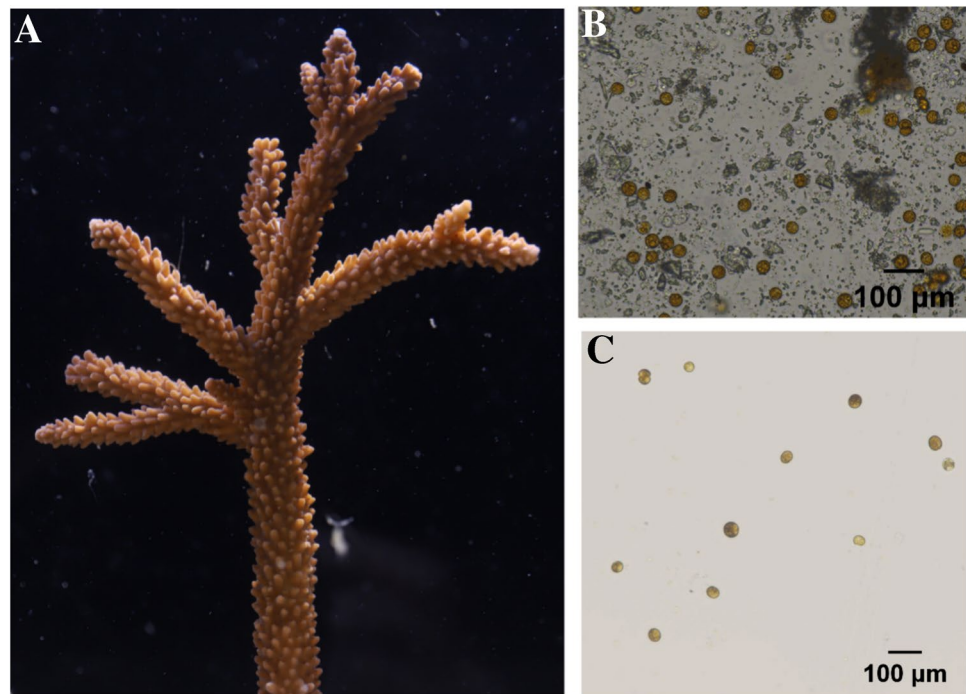
Materials and Methods

Experimental Subjects and Design

C. goreau was isolated from *Acropora formosa* colonies collected from Weizhou Island reef flats (21°N, 109°E; 2–4 m depth) in August 2022. Coral fragments (5–10 cm) were harvested by underwater chiseling, transported in seawater, and air-brushed to extract tissues. During sampling, surface seawater conditions were as follows: temperature = 28.5 ± 0.5 °C, salinity = $35 \pm 1.5\%$, and pH = 8.2 ± 0.1 . Measurements were conducted using the protocols of Qin et al. [28]. Symbiodiniaceae were purified using a discontinuous Percoll density gradient (40%, 60%, and 80% in sterile seawater) followed by centrifugation at $4000 \times g$ for 10 min. The algal layer at the 60–80% interface was collected. The prepared algal suspension was aseptically transferred to 96-well plates containing L1 medium (Supplementary Table 1) and cultured in LED climate chambers (RDN-500D-CO₂) under controlled conditions (50 μ mol photons·m⁻²·s⁻¹, 26 ± 0.5 °C, 12 h:12 h light:dark cycle). The Symbiodiniaceae cultures were subcultured every 2 weeks using a 1:10 dilution method (culture: medium ratio). Weekly growth monitoring was performed using inverted microscopy. Following morphological confirmation as Symbiodiniaceae, Sanger sequencing was conducted to verify their identity as Symbiodiniaceae. To verify the purification efficiency of Symbiodiniaceae, a second round of high-throughput sequencing was performed after 2 months of culture following the initial high-throughput sequencing. The results demonstrated that the relative abundance of *C. goreau* exceeded 90% in both sequencing runs. Detailed sequencing metrics are provided in Supplementary Table 2.

Cell density of *C. goreau* was counted using a hemocytometer (Marienfeld Superior). The cell density of each experimental group was adjusted to 1.1×10^5 cells/mL by adding sterile seawater. Figure 1B and C show the microscopic examination of *C. goreau* under an optical microscope (Nikon, ECLIPSE Ni-E) at $\times 400$ magnification. The experimental temperature gradients were set as follows: high temperature group (26 °C, 29 °C, 32 °C, and 34 °C) and low temperature group (26 °C, 20 °C, and 14 °C), with an initial temperature of 26 °C, each containing three technical replicates. The temperatures are in reference to the extreme temperatures in WI [29]. Technical replicates were defined as triplicate subcultures derived from the same parent *C. goreau* population and maintained in three identical under synchronized conditions. Daily verification was performed

Fig. 1 Cultured *Cladocopium goreaui* were observed under an optical microscope. **A** The *Acropora formosa* symbiotic with *C. goreaui*. **B** Initial isolation of *C. goreaui* from *Acropora formosa*. **C** *C. goreaui* after purification culture



using Traceable® ISO 17025-certified thermometers (± 0.1 °C accuracy). Control samples (ambient temperature, 26 °C) were collected at the experiment's initiation. Temperature adjustments were applied weekly in stepwise increments (Fig. 2). Environmental parameters excluding temperature were standardized across all incubators to eliminate confounding variables. The light intensity of the incubators was uniformly adjusted to 50 μmol photons· $\text{m}^{-2}\cdot\text{s}^{-1}$, the humidity was adjusted to 60% RH, and the CO_2 concentration was adjusted to 500 ppm.

Maximum Quantum Yield (F_v/F_m) and Transmission Electron Microscopy (TEM)

In this study, the F_v/F_m in *C. goreaui* was quantified at all sampling timepoints using a DIVING-PAM Submersible Fluorometer (WalzHeinaGmbh, Effeltrich, Germany). Prior to measurement, symbiont cultures were dark-adapted for > 2 h in lighted incubator. F_m was the maximum chlorophyll fluorescence of dark-adapted cells in the presence of a saturating blue light pulse (3000 μmol photons $\text{m}^{-2}\text{s}^{-1}$, 1 s). F_o was the minimum fluorescence in the presence of a weakly modulated measured light. F_v/F_m [30] was calculated as follows:

$$\frac{F_v}{F_m} = \frac{F_m - F_o}{F_m}$$

Samples of *C. goreaui* were post-fixed in 1% OsO₄/0.1 M phosphate buffer (pH 7.4) for 2 h at RT (dark), rinsed

3 \times 15 min with the same buffer, then dehydrated through an ethanol series (30% \rightarrow 50% \rightarrow 70% \rightarrow 80% \rightarrow 95% \rightarrow 100%, 20 min each) and acetone (2 \times 15 min). Infiltration with EMBed 812 resin followed sequential mixtures: acetone:resin (1:1, 2–4 h; 1:2, overnight) and pure resin (5–8 h) at 37 °C. After embedding and polymerization (37 °C overnight \rightarrow 60 °C, 48 h), ultrathin Sects. (60–80 nm) were mounted on 150-mesh copper grids. Double staining with 2% uranyl acetate (8 min, dark) and 2.6% lead citrate (8 min, CO_2 -free) was performed, with rinses in 70% ethanol and ultrapure water. Grids were air-dried overnight and imaged via TEM (Hitachi HT-7800, 80 kV).

Transcriptome Sequencing and Bioinformatics Analysis

C. goreaui samples from the control group (26 °C), high temperature group (34 °C), and low temperature group (14 °C) were collected for transcriptomic sequencing following temperature treatment. The culture solution containing *C. goreaui* cells was dispensed into 50-mL sterile and enzyme-free centrifuge tubes, vortexed and mixed, and centrifuged using a high-speed cryocentrifuge at 500 $\times g$ for 10 min at 4 °C. The supernatant was aspirated, the cells were washed with PBS two to three times, and the cells were removed from the centrifuge. After removing phosphate-buffered saline by aspiration, pelleted *C. goreaui* cells were transferred to 2-mL cryogenic vials (CORNING, MEX), snap-frozen in liquid nitrogen, and stored at –80 °C until RNA extraction.

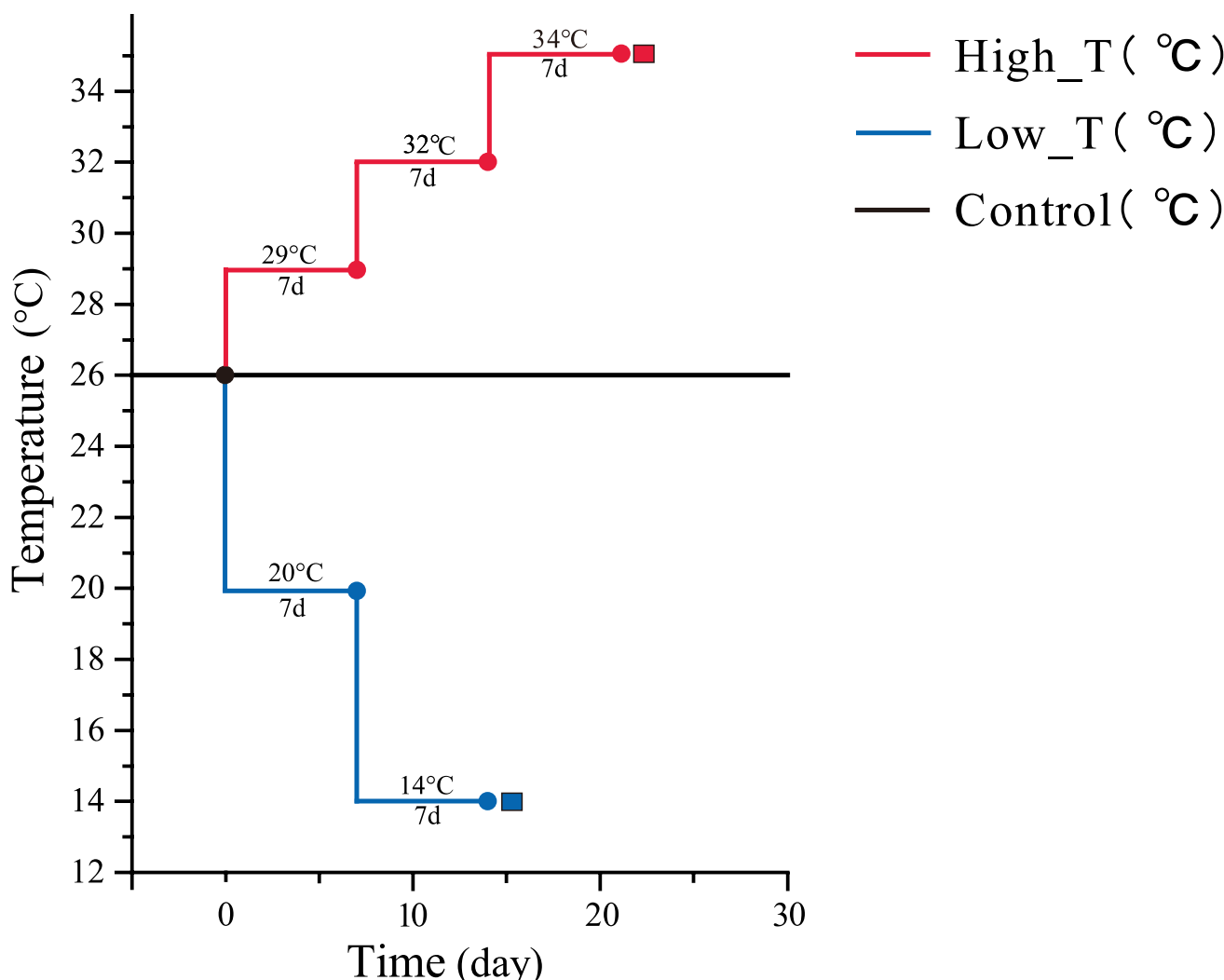


Fig. 2 Experimental temperature settings. Red line represents the high-temperature group ($26\text{ }^{\circ}\text{C}\rightarrow 29\text{ }^{\circ}\text{C}\rightarrow 32\text{ }^{\circ}\text{C}\rightarrow 34\text{ }^{\circ}\text{C}$), black line indicates the control group (constant $26\text{ }^{\circ}\text{C}$), and blue line denotes the low-temperature group ($26\text{ }^{\circ}\text{C}\rightarrow 20\text{ }^{\circ}\text{C}\rightarrow 14\text{ }^{\circ}\text{C}$). Circles mark sam-

pling points for maximum quantum yield of Photosystem II (F_v/F_m). Squares indicate transcriptomic sampling and transmission electron microscopy (TEM) analyses timepoints

Total RNA was extracted from *C. goreau* samples using TRIzol® Reagent (QIAzol Lysis Reagent, Qiagen), with quality control parameters rigorously validated: RNA purity ($A_{260}/A_{280}=1.8\text{--}2.2$; $A_{260}/A_{230}\geq 2.0$) was assessed via NanoDrop ND-2000, while RNA integrity (RQN ≥ 6.5) and ribosomal ratios ($28\text{S}:18\text{S}\geq 1.0$) were confirmed using Agilent 5300 Bioanalyzer (RNA ScreenTape Assay). Poly(A)+mRNA was enriched from 1 μg high-quality RNA and fragmented to 300 ± 50 bp using NEBNext Magnesium RNA Fragmentation Module ($94\text{ }^{\circ}\text{C}$, 8 min). Stranded RNA-seq libraries were constructed with Illumina Stranded mRNA Prep Kit (Cat. 20,040,534), including cDNA synthesis (SuperScript IV Reverse Transcriptase, Invitrogen), end repair, A-tailing, and adapter ligation. Final libraries were validated via Agilent 4200 TapeStation (DNA HS D1000,

insert size 320 ± 25 bp) and sequenced on Illumina NovaSeq X Plus (2×150 bp paired-end) at Majorbio Bio-pharm Biotechnology Co., Ltd.

The raw paired end reads were trimmed and quality controlled by fastp [31] with default parameters. Then, clean reads were separately aligned to reference genome with orientation mode using HISAT2 [32] (<http://ccb.jhu.edu/software/hisat2/index.shtml>) software. The specific filtering procedures are detailed as follows: Adapter sequences were removed from reads, and reads without inserted fragments (e.g., due to adapter self-ligation) were discarded. Low-quality bases (quality score < 20) at the 3' end were trimmed. If any base with a quality score below 10 remained after trimming, the entire read was discarded; otherwise, it was retained. Reads containing $> 10\%$ undetermined bases (N) were eliminated.

Post-trimming reads shorter than 20 bp were excluded. After quality control, filtered data underwent re-evaluation including base error rate distribution analysis and nucleotide content distribution statistics. The filtered clean data were compared with the reference genome *C. goreaui* (<http://sybms.reefgenomics.org/download/>) [33], and the mapped data were used for transcript assembly and expression calculation. The mapped reads of each sample were assembled by StringTie [34] in a reference-based approach. To identify DEGs (differential expression genes) between two different samples, the expression level of each transcript was calculated according to the transcripts per million reads (TPM) method [35]. RSEM [36] was used to quantify gene abundances. Differential expression analysis was performed using the DESeq2 (<http://bioconduct.org/packages/stats/bioc/DESeq2/>). DEGs with $|log2FC| \geq 1$ and $FDR < 0.05$ (DESeq2) or $FDR < 0.001$ (DEGseq) [37] were considered to be significantly different expressed genes. In addition, functional-enrichment analysis including KEGG was performed to identify which DEGs were significantly enriched in metabolic pathways at Bonferroni-corrected P -value < 0.05 compared with the whole-transcriptome background. *C. goreaui* differentially expressed genes were categorized into biological pathways or functional hierarchies using the KEGG Orthology (KO) system via Blast KOALA [38] annotation (sequence-based KO assignment), followed by KEGG Mapper's Reconstruct tool to map K numbers to organism-specific pathways, and enrichment analysis of DEGs through the KEGG PATHWAY database [39]. The KEGG pathway enrichment analysis was performed using the Python SciPy package [40]. To control for the calculation of the false-positive rate, multiple tests were performed using the BH (FDR) method. The corrected P -value was thresholded at 0.05 using Fisher's exact test; the corrected P -value was thresholded and KEGG pathways meeting this condition were defined as those that were significantly enriched in differentially expressed genes [41].

Statistical Analysis

All data are presented as the mean \pm standard deviation of at least three independent technical replicates. Statistical analyses were performed using IBM SPSS Statistics 26 (IBM Corp., Armonk, NY, USA). Differences between groups were assessed by one-way ANOVA using the nonparametric Kruskal–Wallis test, with a P -value < 0.05 considered statistically significant.

Results

Physiological Changes in *C. goreaui* Under Extreme High/Low-Temperature Stress

Kruskal–Wallis analysis showed (Fig. 3) that the *C. goreaui* under ambient temperature (26 °C) exhibited the highest F_v/F_m , indicating intact photosystem II (PSII) function. In contrast, the low-temperature groups (at 20 °C and 14 °C) showed a significant reduction in F_v/F_m ($P = 0.000$), suggesting direct structural damage to PSII. Notably, the high temperature group at 29 °C maintained an F_v/F_m level comparable to that of the ambient temperature (26 °C) ($P = 0.146$), while the groups at 32 °C presented marked declines in F_v/F_m ($P = 0.002$). F_v/F_m became undetectable when the temperature reached 34 °C. The raw F_v/F_m data and statistical analysis results can be found in Supplementary Material 3.

Ultrastructure of *C. goreaui* Under Extreme High/Low-Temperature Stress

In Fig. 4, TEM revealed that under the ambient temperature (26 °C), *C. goreau* cells (8–13 μ m) exhibited intact ultrastructure with pyrenoid-containing chloroplasts surrounded by starch granules. *C. goreau* in the low temperature group

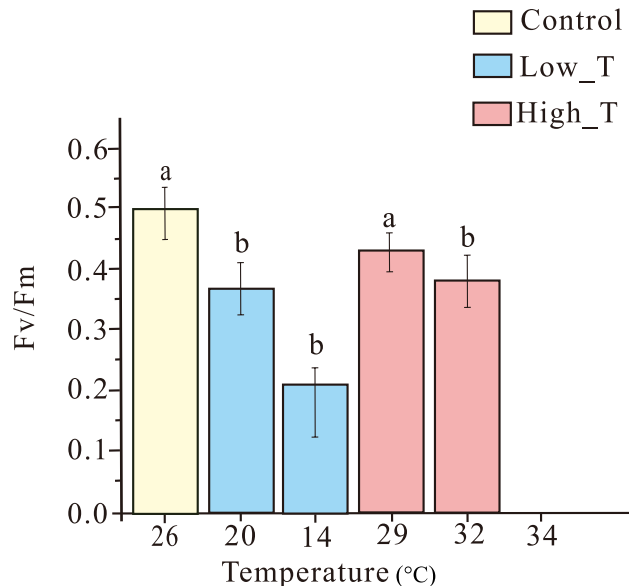


Fig. 3 F_v/F_m activity in *C. goreau* under experimental treatments. Control (maintained at 26 °C), Low_T (exposed to 14 °C and 20 °C for 7 days), and High_T (exposed to 29 °C, 32 °C and 34 °C for 7 days) are represented by yellow, blue, and red, respectively. Different lowercase letters (a, b) above the bars indicate statistically significant differences. F_v/F_m values could not be detected due to severe disruption of thylakoid membranes within chloroplasts at 34 °C

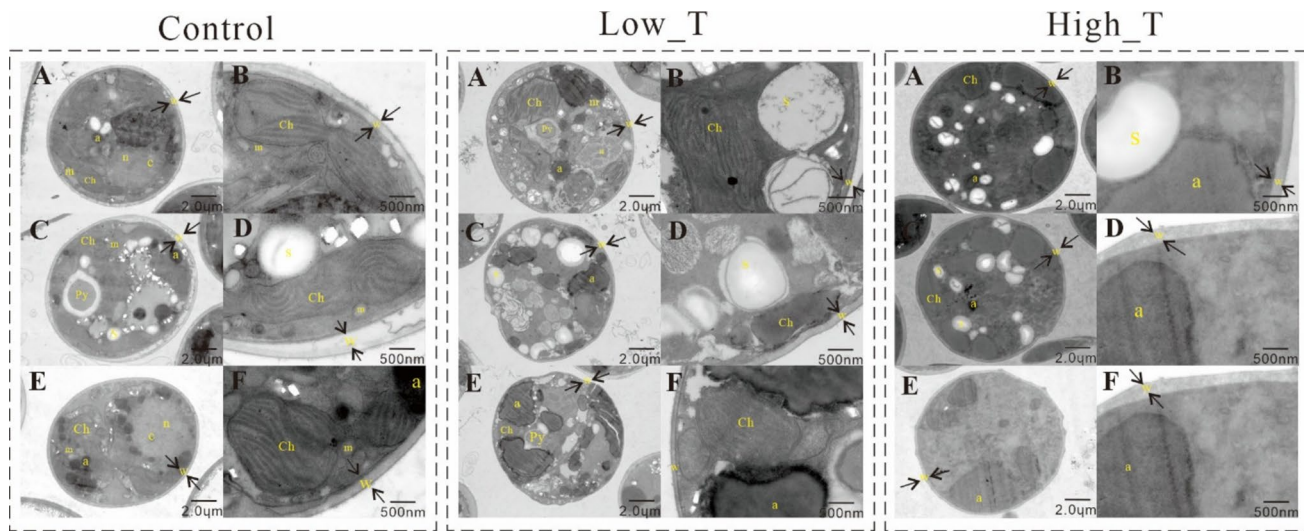


Fig. 4 TEM results of *C. goreau* under different experimental treatment groups. The experimental groups included: Control (maintained at 26 °C), High-T (exposed to 34 °C for 7 days), and Low-T (exposed

to 14 °C for 7 days). “n,” nucleus; “Ch,” chloroplast; “m,” mitochondrion; “s,” starch; “a,” accumulation body; “w,” cell wall; “Py,” pyrenoid; “v,” chromosome

(14 °C) initially showed stress responses. Although the cell wall still existed, the spatial relationship between the cell and the cell wall might have undergone subtle changes, such as a slight trend of plasmolysis. The internal structure of the chloroplast gradually became disordered, and the arrangement of thylakoids was distorted, which seriously threatened the progress of the light-dependent reaction in photosynthesis. *C. goreau* in the high temperature group (34 °C) suffered more severe damage. Apoptotic characteristics were significant, and the physiological functions of the cells were on the verge of collapse. The abnormal accumulation of starch revealed the blockage of the pathway for the conversion and utilization of photosynthesis products. A large number of thylakoids in chloroplasts were lost, and photosynthesis was basically paralyzed. The spatial changes between the cell wall and the cells were exacerbated, and the cell morphology was severely distorted.

Transcriptome Analysis of *C. goreau* Under Extreme High/Low-Temperature Stress

RNA-seq generated 74.13 Gb clean data (> 7.4 Gb per group), with Q30 scores > 92.18% indicating > 99.9% base-call accuracy. The percentage of clean reads mapped to the designated reference genome ranged from 75.86% to 78.0% across samples (Supplementary Table 4).

The Venn diagram (Fig. 5A) identified 21,400 shared genes among control group (26 °C), high temperature group (34 °C), and low temperature group (14 °C) with 67, 342, and 243 group specific genes, respectively, indicating overlapping and unique temperature responses to guide KEGG analysis. PCA (Fig. 5B) revealed PC1 (43.6%) and

PC2 (31.82%) collectively explained 75.42% of variance, visualizing major expression differences and separating experimental groups most distinctly high temperature group (34 °C) vs control group (26 °C) confirming significant temperature impacts on *C. goreau*. Tight intra-group clustering in PCA demonstrated strong technical reproducibility. Correlation heatmap (Fig. 5C) further validated replicate consistency (intra-group $R^2 > 0.98$, dark red), excluding technical artifacts. Table 1 summarizes DEGs under temperature stress. The High-T group exhibited 2831 DEGs ($P < 0.05$, $\log_2FC \geq 1$), comprising 2364 upregulated and 467 downregulated genes. The Low-T group showed 2774 DEGs, with 1498 significantly upregulated and 1249 downregulated genes. Complete datasets are provided in Supplementary Tables 5 and 6.

KEGG analysis revealed temperature-dependent pathway shifts: at 34 °C, upregulation biosynthesis of various plant secondary metabolites, arginine and proline metabolism, nucleocytoplasmic transport, fatty acid biosynthesis, propanoate metabolism, and tryptophan metabolism pathway (Fig. 6A), while downregulation protein processing in endoplasmic reticulum, ascorbate and aldarate metabolism, ribosomes, pentose and glucuronate interconversions, phagosome, and porphyrin metabolism pathway (Fig. 6B) (P value < 0.05). Among these, the differentially expressed genes UGT/DHx38 were significantly downregulated in the ascorbate and aldarate metabolism pathway, while HSP90A and HSP90B were significantly downregulated in the protein processing in endoplasmic reticulum pathway. At 14 °C, spliceosome, mRNA surveillance, nucleocytoplasmic transport, and ribosome biogenesis in eukaryotes pathway were upregulated (Fig. 6C), but glutathione

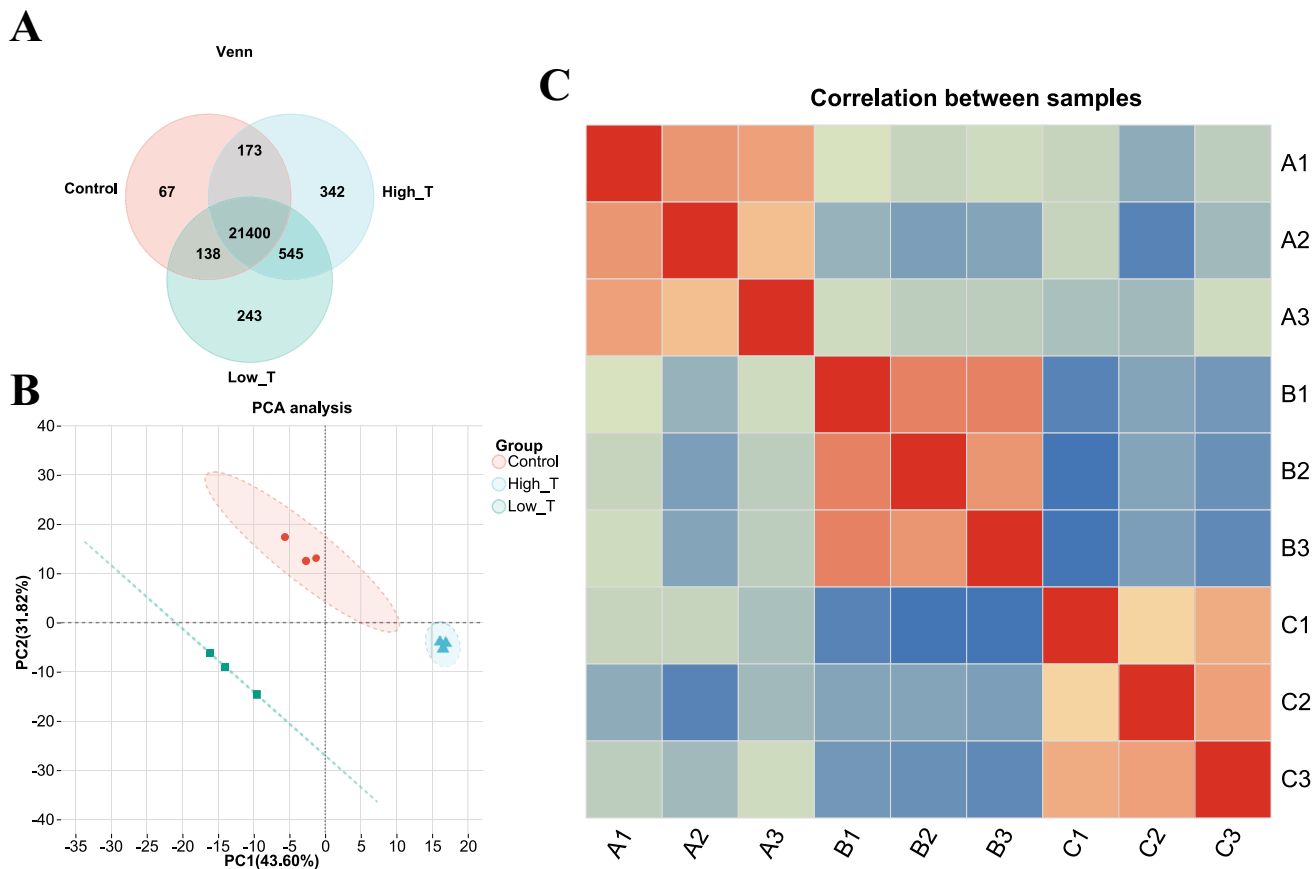


Fig. 5 Correlation and differentially expressed gene analysis of the expression level of *C. goreaui* transcriptome under high/low-temperature stress. **A** Venn diagram of the number of *C. goreaui* specific and shared genes in different experimental groups. **B** PCA analysis of the expression levels of *C. goreaui* transcriptomes in different experi-

mental groups. **C** Graph of correlation analysis between different experimental groups based on the *C. goreaui*'s transcriptomes. Control (maintained at 26 °C), High-T (exposed to 34 °C for 7 days), and Low-T (exposed to 14 °C for 7 days)

Table 1 Different expression gene numbers among groups of *C. goreaui* under extreme high/low-temperature stress

Group	Significantly differentially expressed genes	Upregulated DEGs	Downregulated DEGs
High_T_vs_Control	2831	2364	467
Low_T_vs_Control	2747	1498	1249

metabolism and protein processing in endoplasmic reticulum pathway downregulated (Fig. 6D) (P value < 0.05). Among these, the differentially expressed gene GST was significantly downregulated in the glutathione metabolism pathways, while HSP90B and HSPBP1 were significantly downregulated in the protein processing in endoplasmic reticulum pathway. Supplementary Table 7 includes KEGG pathway analysis of differentially expressed genes (DEGs) under difference stress.

Discussion

Multidimensional Response Mechanisms of Photosynthetic Function and Metabolic Pathways in *C. goreaui* Under High Temperature Stress

Temperature stress affects the physiological state of Symbiodiniaceae. Elevated temperatures perhaps disrupt electron transfer in the photosynthetic system, reducing the F_v/F_m and ultimately impairing photosynthetic efficiency [42]. As shown in Fig. 3A, F_v/F_m at 29 °C showed no significant difference from the control group (26 °C). After 32 °C, F_v/F_m decreased sharply, identifying 32 °C as the critical threshold for PSII heat damage, and at 34 °C, F_v/F_m was undetectable. Howells et al. (2011) demonstrated that Symbiodinium C1 shows no stress at 32 °C after 11 days, with F_v/F_m 16% higher than controls (27 °C), and a follow-up study confirmed stable photosynthetic performance and exROS levels after 15 days at 32 °C [26]. The F_v/F_m of *C. goreaui* remains stable at 29 °C, likely reflecting its short-term

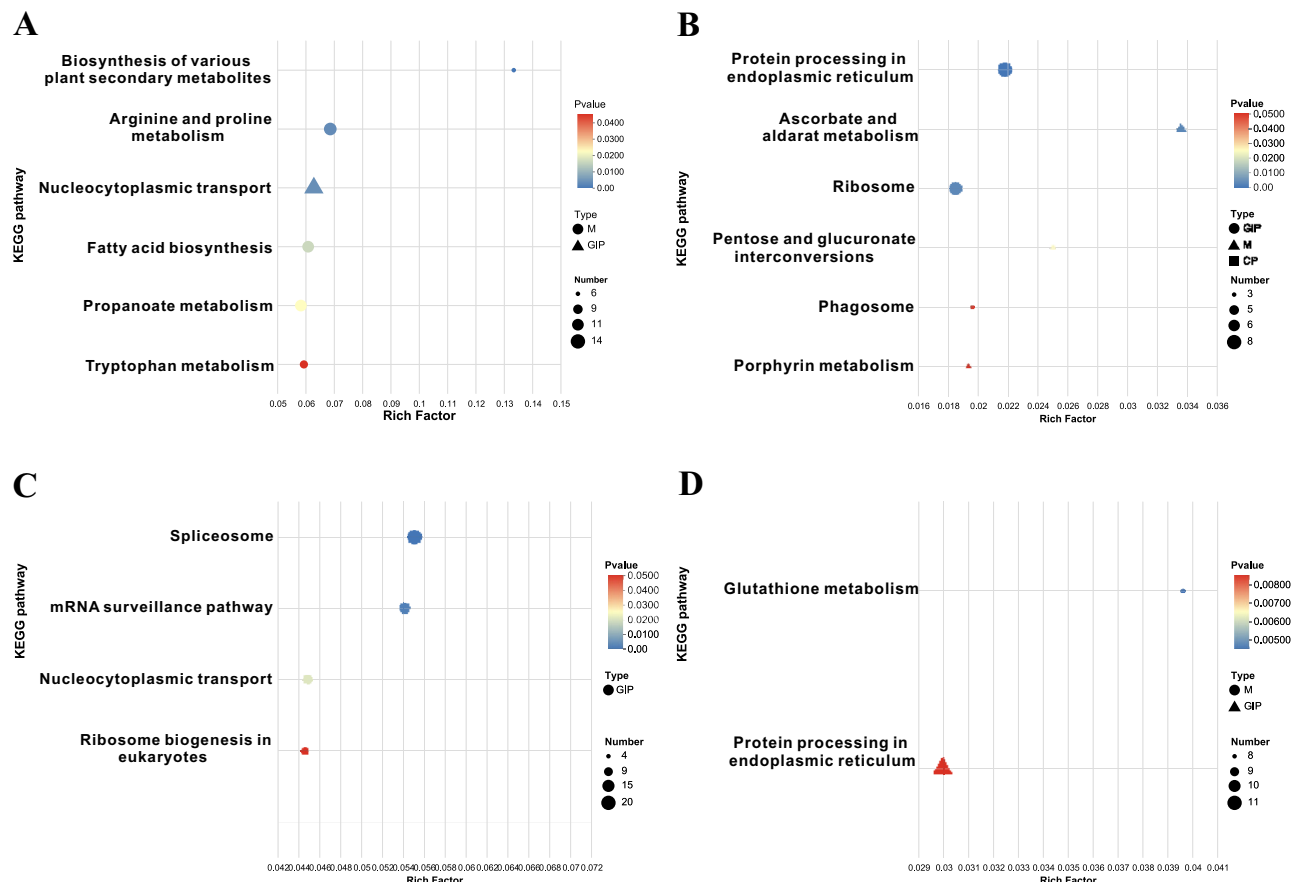


Fig. 6 KEGG enrichment analysis plot of differentially expressed genes. **A** Enrichment results of significantly upregulated genes in the high-temperature group. **B** Enrichment results of significantly downregulated genes in the high-temperature group. **C** Enrichment results of significantly upregulated genes in the low-temperature group. **D** Enrichment results of significantly downregulated genes in the low-temperature group. The y-axis displays pathway names, while the

x-axis represents the Rich factor (defined as the ratio of enriched genes in the pathway to the annotated background genes). Larger Rich factors indicate stronger enrichment. The size of each point corresponds to the number of genes in the pathway, and the color denotes different ranges of adjusted *p*-values. M, metabolism; GIP, genetic information processing; CP, cellular process

thermal acclimation capacity, which is consistent with the performance of corals in high-latitude regions. There, seasonal temperature fluctuations have selected for physiological plasticity in coral responses to temperature stress within marginal coral communities [43]. In contrast, *Symbiodinium* C1 can enhance F_v/F_m at 32 °C, suggesting that tropical symbionts may have evolved constitutive heat tolerance to persist in stable, warm environments [26]. The divergence between *C. goreaui* and *Symbiodinium* C1 also underscores the potential for “symbiont shuffling” in high-latitude corals. If warming exceeds *C. goreaui*’s threshold, corals may switch to more heat-tolerant symbionts (e.g., *Durusdinum*), as observed in tropical systems [26, 44]. Structurally, thylakoid membranes—embedded in the chloroplast stroma and densely distributed around the pyrenoid—are central to light energy capture [45]. TEM images of the high temperature group (Fig. 4) revealed *C. goreaui* thylakoid membrane disintegration and loss of light energy capture efficiency. This

structural collapse likely explains the undetectable F_v/F_m at 34 °C [46].

High temperature stress increases the concentration of ROS in Symbiodiniaceae cells [47]. High concentration ROS interacts with components involved in mitochondrial apoptosis, which promotes cell apoptosis [48]. In eukaryotic cells, superoxide dismutase (SOD) is one of the important anti-oxidant pathways, providing the first line of defense against O_2^- and H_2O_2 and alleviating the damage caused by ROS to cells [49]. KEGG enrichment analysis revealed a significant upregulation of arginine and proline metabolism pathways in the high-temperature group. These two nitrogen-containing compounds are not only important osmoregulators but also can indirectly enhance ROS scavenging capacity by participating in the glutathione cycle [50]. Polyamines derived from arginine can stabilize thylakoid membrane structures, while proline directly scavenges hydroxyl radicals ($\cdot OH$) and assists SOD in coping with the explosive accumulation of

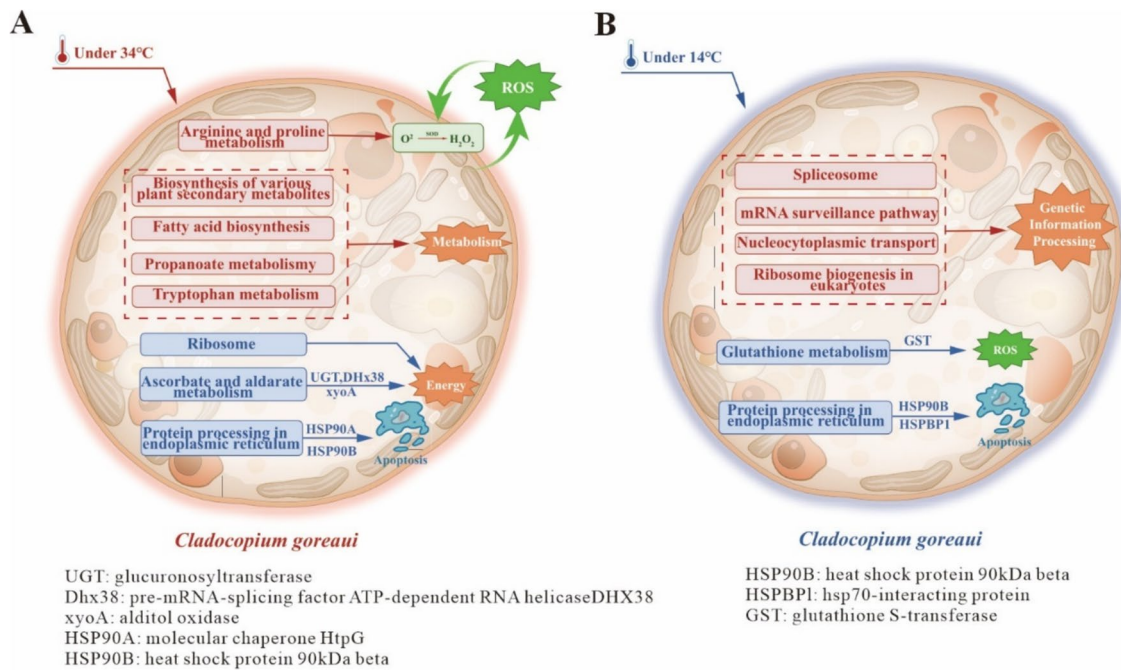


Fig. 7 Response mechanisms of *C. goreau* at different temperatures. **A** High temperature at 34 °C. **B** Low temperature at 14 °C. Color types indicate *C. goreau* upregulated (red) and downregulated (blue) expression

O_2^- and H_2O_2 , thereby delaying the vicious cycle of oxidative damage → photosynthetic collapse [51].

High temperature may induce apoptosis in *C. goreau* cells [52]. KEGG enrichment analysis shows that the protein processing in endoplasmic reticulum pathway in dinoflagellate symbionts was significantly downregulated, indicating that the cells were reducing protein synthesis [53]. Within the ER protein processing pathway, the significant downregulation of HSP90A and HSP90B represents a critical tipping point for apoptosis in *C. goreau*. HSP90 is a conserved molecular chaperone with dual roles: maintaining the stability of client proteins (e.g., signaling kinases, transcription factors) and directly inhibiting apoptotic signaling [54]. Studies have shown differential expression patterns of HSP70 and HSP90 in coral hosts and their algal symbionts under heat stress. In *Acropora aspera*, coral HSP90 and HSP70 were significantly upregulated during bleaching, while symbiont HSP90 decreased [55]. Similarly, in *Symbiodinium*, moderate heat stress increased HSP70 expression, but extreme stress reduced it, while HSP90 expression decreased under all heat stress conditions [54]. In coral symbionts, HSP90 upregulation is typically associated with thermal tolerance—for example, tropical *Durusdinium* strains upregulate HSP90 to protect photosynthetic machinery under heat stress [56]. In this study, downregulation of heat shock proteins may lead to apoptosis in *C. goreau* [57].

High-temperature stress critically disrupts *C. goreau* metabolism and survival, triggering upregulation of five

protective metabolic pathways—biosynthesis of plant secondary metabolites, fatty acid biosynthesis, propanoate metabolism, arginine and proline metabolism, and tryptophan metabolism—which enhance osmoprotection, membrane integrity, and antioxidant capacity as observed in analogous heat-stressed phototrophs like seaweed *Pyropia haitanensis* [58]. Concurrently, *C. goreau* counteracts energy metabolism disorder [59] by downregulating energy-intensive processes (e.g., ribosome biogenesis and ascorbate/aldarate metabolism) [60], while redirecting carbon flux through UGT/xyoA-catalyzed pentose/glucuronate interconversions to optimize TCA cycle efficiency for ATP homeostasis. This dual strategy of protective metabolite induction and precision energy governance, aligned with proteomic-documented prioritization of photosynthesis and defense over protein synthesis [61], sustains cellular function under thermal extremes. For high-latitude coral reefs dominated by *C. goreau*, this metabolic flexibility provides partial buffering against climate change. Upregulation of stress pathways may extend survival during transient heatwaves, consistent with predictions that temperate reefs could serve as climate refugia [62]. Notably, this metabolic profile contrasts sharply with tropical symbionts (e.g., *Durusdinium*), which typically upregulate energy-intensive pathways such as oxidative phosphorylation to enhance antioxidant defenses [56]. This divergence likely reflects adaptation to distinct thermal regimes: tropical symbionts prioritize sustained defense in stable, warm environments, whereas high-latitude *C. goreau*

prioritizes plastic energy conservation to survive seasonal fluctuations (Fig. 7).

Energy Reallocation in Cold-Stressed *C. goreau*: Prioritize Genetic Fidelity

Low-temperature stress, as a non-negligible abiotic disturbance factor in the marine environment, exerts a remarkable remodeling effect on the physiological homeostasis of coral symbiotic Symbiodiniaceae [63]. Figure 3 shows that the F_v/F_m in the 20 °C and 14 °C groups was significantly lower than that in the control group, reflecting the blockage of the photosynthetic electron transport chain [64]. The phenomenon of thylakoid disintegration was observed from the TEM results, which may be the reason for the significant decrease in F_v/F_m [46]. In addition to photosynthetic damage, low temperature stress may also inhibit the antioxidant defense capacity of *C. goreau*, rendering cells vulnerable to the accumulation of ROS [65]. KEGG enrichment analysis shows that the glutathione metabolic pathway was significantly downregulated, and the gene GST related to the glutathione metabolic pathway was also significantly downregulated. Glutathione plays a crucial role in the cellular antioxidant system. GST is a key enzyme in glutathione metabolism, which can accelerate glutathione synthesis, and reduced glutathione can counteract ROS [66]. This indicates that *C. goreau* may have defects in the enzymatic antioxidant pathway. This stands in sharp contrast to *C. goreau*'s response to heat stress, where arginine/proline metabolism is upregulated to enhance ROS scavenging.

Low-temperature stress poses unique challenges to cellular integrity, affecting various aspects of genetic information transfer. Cold denaturation can alter protein structure at quaternary, tertiary, and secondary levels, leading to cellular injuries [67]. Eukaryotic cells respond to hypothermia through various regulatory mechanisms, including alterations in gene expression, attenuated protein synthesis, and changes in lipid composition, to preserve energy and prolong cell survival [68]. In our study, KEGG enrichment analysis revealed that *C. goreau* significantly upregulated four pathways related to genetic information processing: the spliceosome pathway, mRNA surveillance pathway, nucleocytoplasmic transport, and ribosome biogenesis in eukaryotes. While downregulating the endoplasmic reticulum protein processing pathway. The spliceosome repairs pre-mRNA splicing errors to ensure the correct expression of cold-responsive genes [69]. The mRNA surveillance pathway degrades abnormal mRNA, thereby maintaining transcriptome quality [70]. Nucleocytoplasmic transport accelerates the nuclear import of stress factors and the export of mature mRNA, safeguarding the continuity of gene expression [71]. Ribosome biogenesis in eukaryotes optimizes ribosome assembly to support the translation of key proteins [72].

Collectively, the upregulation of these pathways indicates that *C. goreau* prioritizes ensuring the fidelity of genetic information flow over protein-dependent repair mechanisms (e.g., heat shock proteins) under cold stress. This emphasis on genetic repair stands in sharp contrast to *C. goreau*'s response to heat stress, where protein-dependent defenses are prioritized.

ER stress may trigger cell death [73]. Under cold stress, *C. goreau* exhibits ER stress characterized by downregulation of protein processing pathways within the ER [74]—a critical system for cellular protein synthesis and modification. Specifically, key heat shock protein (HSP) genes (HSP90B and HSPBP1) in this pathway are significantly suppressed. Notably, HSPs play essential roles in stabilizing protein folding, preventing aggregation, and facilitating stress response under abiotic challenges including cold [75]. This coordinated downregulation likely reflects *C. goreau*'s adaptive resource reallocation strategy: redirecting energy from protein processing toward cold adaptation mechanisms. While this prioritization may temporarily sustain cellular function, it carries trade-offs—insufficient chaperone activity that may trigger apoptotic pathways under extreme cold stress [76]. High-latitude coral reefs experience seasonal cold snaps but return to optimal temperatures annually [77]. Under cold stress, *C. goreau* regulates genetic information processing while suppressing ER protein processing, demonstrating its resource allocation strategy under energy-limited conditions. By prioritizing the fidelity of genetic information flow, it ensures survival during cold exposure (Fig. 7).

Conclusion

Temperature stress significantly impacts the physiological state of *C. goreau*, disrupting photosynthetic electron transfer and reducing F_v/F_m , thereby impairing photosynthetic efficiency. At 29 °C, F_v/F_m remains comparable to the control (26 °C), but beyond 32 °C—a critical threshold for PSII damage—it declines sharply, becoming undetectable at 34 °C. While *Symbiodinium* C1 exhibits thermal tolerance at 32 °C, *C. goreau* demonstrates short-term acclimation at 29 °C, reflecting adaptations to seasonal fluctuations in high-latitude reefs. Structural damage to thylakoid membranes at high temperatures explains the photosynthetic collapse. Concurrently, heat stress elevates ROS levels, triggering apoptosis, though antioxidant pathways (e.g., arginine/proline metabolism) and metabolic adjustments (e.g., downregulation of energy-intensive processes) partially mitigate damage. In contrast, cold stress (14–20 °C) impairs photosynthesis and antioxidant capacity (e.g., glutathione downregulation), while *C. goreau*

prioritizes genetic fidelity via upregulated spliceosome and mRNA surveillance pathways, sacrificing protein repair mechanisms. This divergence in stress responses underscores *C. goreau*'s adaptive strategies: metabolic flexibility for heat and genetic preservation for cold, aligning with its niche in thermally variable reefs.

Supplementary Information The online version contains supplementary material available at <https://doi.org/10.1007/s00248-025-02587-0>.

Acknowledgements This research was supported by the National Natural Science Foundation of China (42206157, 42030502, 42090041), the Natural Science Foundation of Guangxi Province (2025GXNSFAA069187). The authors declare that the research was conducted in the absence of any commercial or financial relationships that could be construed as a potential conflict of interest. The raw data were deposited in the NCBI Sequence Read Archive (SRA) database (<https://www.ncbi.nlm.nih.gov/>, PRJNA1245310).

Author Contribution Author Contributions Statement LFW (First Author): Conceptualization, Methodology, Formal Analysis, Writing—Original Draft; SCC: Data Curation, Software, Validation; ZJQ(Corresponding Author): Methodology, Formal Analysis, Visualization; Writing—Review & Editing, Funding Acquisition; NBP: Formal Analysis, Writing—Review & Editing; MLL: Software Development, Data Visualization; TCZ: Formal Analysis, Supervision; RH: Methodology, Validation, Writing—Review & Editing; HYL: Data Collection, Visualization; WZD: Supervision, Writing—Review & Editing; CHM: Formal Analysis, Statistical Analysis; KFY (Corresponding Author): Conceptualization, Funding Acquisition, Supervision, Writing—Review & Editing, Project Administration. All authors have reviewed and approved the final version of the manuscript.

Funding This research was supported by the National Natural Science Foundation of China (42206157, 42030502, 42090041), the Natural Science Foundation of Guangxi Province (2025GXNSFAA069187).

Data Availability The raw data were deposited in the NCBI Sequence Read Archive (SRA) database (<https://www.ncbi.nlm.nih.gov/>, PRJNA1245310).

Declarations

Competing Interests The authors declare no competing interests.

Open Access This article is licensed under a Creative Commons Attribution-NonCommercial-NoDerivatives 4.0 International License, which permits any non-commercial use, sharing, distribution and reproduction in any medium or format, as long as you give appropriate credit to the original author(s) and the source, provide a link to the Creative Commons licence, and indicate if you modified the licensed material. You do not have permission under this licence to share adapted material derived from this article or parts of it. The images or other third party material in this article are included in the article's Creative Commons licence, unless indicated otherwise in a credit line to the material. If material is not included in the article's Creative Commons licence and your intended use is not permitted by statutory regulation or exceeds the permitted use, you will need to obtain permission directly from the copyright holder. To view a copy of this licence, visit <http://creativecommons.org/licenses/by-nc-nd/4.0/>.

References

- Voolstra CR, Suggett DJ, Peixoto RS et al (2021) Extending the natural adaptive capacity of coral holobionts. *Nat Rev Earth Environ* 2(11):747–762. <https://doi.org/10.1038/s43017-021-00214-3>
- Lajeunesse TC, Everett PJ, Gabrielson PW et al (2018) Systematic revision of Symbiodiniaceae highlights the antiquity and diversity of coral endosymbionts. *Curr Biol* 28:2570–2580. <https://doi.org/10.1016/j.cub.2018.07.008>
- Zhang M, Huang S, Luo L (2015) Environmental acclimatization of the relatively high latitude scleractinian coral *Pavona decussata*: integrative perspectives on seasonal subaerial exposure and temperature fluctuations. *BMC Genomics* 26(1):483. <https://doi.org/10.1186/s12864-025-11660-4>
- Hughes Terry P, Kerry James T, Álvarez-Noriega M et al (2017) Global warming and recurrent mass bleaching of corals. *Nature* 543(7645):373–377. <https://doi.org/10.1038/nature21707>
- Chakravarti LJ, Beltran VH, Van Oppen MJH (2017) Rapid thermal adaptation in photosymbionts of reef-building corals. *Glob Change Biol* 10:40. <https://doi.org/10.1111/gcb.13702>
- Murata N, Takahashi S, Nishiyama Y et al (2007) Photoinhibition of photosystem II under environmental stress. *Biochimica et Biophysica Acta (BBA)-Bioenergetics* 1767(6):414–421. <https://doi.org/10.1016/j.bbabi.2006.11.019>
- Wang Q L, Chen J H, He N Y (2018) Metabolic reprogramming in chloroplasts under heat stress in plants. *Int J Mol Sci* 2018. 19(3). <https://doi.org/10.3390/ijms19030849>
- Marangoni L F D B, C Rottier, C Ferrier-Pagès (2021) Symbiont regulation in *Stylophora pistillata* during cold stress: an acclimation mechanism against oxidative stress and severe bleaching. *J Experimental Biol* 224(Pt 3). <https://doi.org/10.1242/jeb.235275>
- Solayan A (2016) Biomonitoring of coral bleaching - a glimpse on biomarkers for the early detection of oxidative damages in corals, in *Invertebrates - experimental models in toxicity screening*, M.L. Larramendy and S. Soloneski, Editors. 2016, IntechOpen: Rijeka. <https://doi.org/10.5772/61831>
- Yao Y, Wang C (2022) Marine heatwaves and cold-spells in global coral reef zones. *Prog Oceanogr*. <https://doi.org/10.1016/j.pocean.2022.102920>
- Thornhill Daniel J, Kemp Dustin W, Bruns Brigitte U et al (2010) Correspondence between cold tolerance and temperate biogeography in a western Atlantic Symbiodinium (Dinophyta) Lineage1. *J Phycol* 44(5):1126–1135. <https://doi.org/10.1111/j.1529-8817.2008.00567.x>
- Smith D, Suggett D, Baker N (2005) Is photoinhibition of zooxanthellae photosynthesis the primary cause of thermal bleaching in corals? *Global Change Biol. Global Change Biol* 11:1–11. <https://doi.org/10.1111/j.1529-8817.2003.00895.x>
- Shaohua Mo, Tianran C, Zesheng C et al (2022) Marine heatwaves impair the thermal refugia potential of marginal reefs in the northern South China Sea. *Sci Total Environ* 825:154100. <https://doi.org/10.1016/j.scitotenv.2022.154100>
- Tom B, Legorreta F, Mitch RB et al (2014) Variable responses of benthic communities to anomalously warm sea temperatures on a high-latitude coral reef. *PLoS One* 9:e113079. <https://doi.org/10.1371/journal.pone.0113079>
- Wei X, Yu K, Qin Z et al (2024) The acute and chronic low-temperature stress responses in *Porites lutea* from a relatively high-latitude coral reef of the South China Sea. <https://doi.org/10.3389/fmars.2024.1321865>
- Schleyer Michael H, Laing FC, Stuart CS et al (2018) What can South African reefs tell us about the future of high-latitude coral systems? *Mar Pollut Bull* 136:491–507. <https://doi.org/10.1016/j.marpolbul.2018.09.014>

17. Denis V, Mezaki T, Tanaka K et al (2013) Coverage, diversity, and functionality of a high-latitude coral community (Tatsukushi, Shikoku Island, Japan). *PLoS One* 8(1):e54330. <https://doi.org/10.1371/journal.pone.0054330>
18. Chen Tianran, Yu Kefu (2014) Responses and high-resolution records for marine environment changes in the relatively high-latitude corals from the South China Sea[J]. *Quaternary Sciences*, 34(6): 1288-1295<https://doi.org/10.3969/j.issn.1001-7410.2014.06.18>
19. Wang Y, Yu K, Chen X et al (2020) An approach for assessing ecosystem-based adaptation in coral reefs at relatively high latitudes to climate change and human pressure. *Environ Monit Assess* 192:579. <https://doi.org/10.1007/s10661-020-08534-5>
20. Huang W, Yang E, Yu K et al (2022) Lower cold tolerance of tropical *Porites lutea* is possibly detrimental to its migration to relatively high latitude refuges in the South China Sea. *Mol Ecol* 31(20):5339–5355. <https://doi.org/10.1111/mec.16662>
21. YU Kefu, Jiang Mingxing, Cheng Zhiqiang et al (2004) Latest forty two years' sea surface temperature change of Weizhou Island and its influence on coral reef ecosystem. 15(3): 506–510. <https://www.cjae.net/EN/Y2004/V13/506>
22. Yu K (2012) Coral reefs in the South China Sea: their response to and records on past environmental changes. *Sci China Earth Sci*. <https://doi.org/10.1007/s11430-012-4449-5>
23. Nunn Brook L, Tanya B, Emma T-S et al (2025) Protein signatures predict coral resilience and survival to thermal bleaching events. *Commun Earth Environ* 6(1):191. <https://doi.org/10.1038/s43247-025-02167-7>
24. Levin RA, Beltran VH, Hill R et al (2016) Sex, scavengers, and chaperones: transcriptome secrets of divergent *Symbiodinium* thermal tolerances. *Mol Biol Evol* 33(9):2201–2215. <https://doi.org/10.1093/molbev/msw119>
25. McGinty ES, Pieczonka J, Mydlarz LD (2012) Variations in reactive oxygen release and antioxidant activity in multiple *Symbiodinium* types in response to elevated temperature. *Microb Ecol* 64(4):1000–1007. <https://doi.org/10.1007/s00248-012-0085-z>
26. Howells E J Beltran, V H Larsen N W et al (2012) Coral thermal tolerance shaped by local adaptation of photosymbionts. *Nat Climate Change* 2(2): 116-120<https://doi.org/10.1038/nclimate1330>
27. Chen B, Yu K, Liang J et al (2019) Latitudinal variation in the molecular diversity and community composition of *Symbiodiniaceae* in coral from the South China Sea. *Front Microbiol* 10. <https://doi.org/10.3389/fmicb.2019.01278>
28. Qin, Zhenjun, Yu, Kefu, Liang, Jiayuan et al (2020) Significant changes in microbial communities associated with reef corals in the southern South China Sea during the 2015/2016 global-scale coral bleaching event. *J Geophysical Res Oceans* 125. <https://doi.org/10.1029/2019JC015579>
29. Feng Y, Bethel BJ, Dong C et al (2022) Marine heatwave events near Weizhou Island, Beibu Gulf in 2020 and their possible relations to coral bleaching. *Sci Total Environ* 823:153414. <https://doi.org/10.1016/j.scitotenv.2022.153414>
30. Van KO, Snel JF (1990) The use of chlorophyll fluorescence nomenclature in plant stress physiology. *Photosynth Res* 25(3):147–150. <https://doi.org/10.1007/bf00033156>
31. Chen S, Zhou Y, Chen Y et al (2018) fastp: an ultra-fast all-in-one FASTQ preprocessor. *Bioinformatics* 34(17):i884–i890. <https://doi.org/10.1093/bioinformatics/bty560>
32. Kim D, Paggi J, M Park C et al (2019) Graph-based genome alignment and genotyping with HISAT2 and HISAT-genotype. *Nat Biotechnol* 37(8): 907-915<https://doi.org/10.1038/s41587-019-0201-4>
33. Liew Y J, M Aranda, and C R Voolstra (2016) Reefgenomics.Org - a repository for marine genomics data. *Database J Biological Databases Curation*. <https://doi.org/10.1093/database/baw152>
34. Pertea M, Pertea G, Antonescu C et al (2015) Stringtie enables improved reconstruction of a transcriptome from RNA-seq reads. *Nat Biotechnol* 33:290–295. <https://doi.org/10.1038/nbt.3122>
35. In H L Y, and R Pincket (2022)Transcripts per million ratio: applying distribution-aware normalisation over the popular TPM method. <https://doi.org/10.48550/arXiv.2205.02844>
36. Li B, Dewey CN (2011) RSEM: accurate transcript quantification from RNA-Seq data with or without a reference genome. *BMC Bioinformatics* 12(1):323. <https://doi.org/10.1186/1471-2105-12-323>
37. Love MI, Huber W, Anders S (2014) Moderated estimation of fold change and dispersion for RNA-seq data with DESeq2. *Genome Biol* 15(12):550. <https://doi.org/10.1186/s13059-014-0550-8>
38. Kanehisa M, Sato Y, Morishima K (2016) BlastKOALA and GhostKOALA: KEGG tools for functional characterization of genome and metagenome sequences. *J Mol Biol* 428(4):726–731. <https://doi.org/10.1016/j.jmb.2015.11.006>
39. Kanehisa M, Goto S (2000) KEGG: Kyoto Encyclopedia of Genes and Genomes. *Nucleic Acids Res* 28(1):27–30. <https://doi.org/10.1093/nar/gkw1092>
40. Virtanen P, Gommers R, Oliphant TE et al (2020) SciPy 1.0: fundamental algorithms for scientific computing in Python. *Nat Methods* 17:261–272. <https://doi.org/10.1038/s41592-019-0686-2>
41. Chen Xie 1, Xizeng Mao, Jiaju Huang et al (2011) KOBAS 2.0: a web server for annotation and identification of enriched pathways and diseases. *Nucleic Acids Research*. 39(Web Server issue) 316–22. <https://doi.org/10.1093/nar/gkr483>
42. Warner ME, Fitt WK, Schmidt GW (1996) The effects of elevated temperature on the photosynthetic efficiency of zooxanthellae in hospite from four different species of reef coral: a novel approach. *Plant Cell Environ* 19:291–299. <https://doi.org/10.1111/j.1365-3040.1996.tb00251.x>
43. Keshavmurthy S, Beals M, Hsieh HJ et al (2021) Physiological plasticity of corals to temperature stress in marginal coral communities. *Sci Total Environ* 758:143628. <https://doi.org/10.1016/j.scitotenv.2020.143628>
44. Abbott E, Dixon G, Matz M (2021) Shuffling between *Cladocodium* and *Durusdinium* extensively modifies the physiology of each symbiont without stressing the coral host. *Mol Ecol* 30(24):6585–6595. <https://doi.org/10.1111/mec.16190>
45. Zhao LS, Huokko T, Wilson S et al (2020) Structural variability, coordination and adaptation of a native photosynthetic machinery. *Nat Plants* 6:869–882. <https://doi.org/10.1038/s41477-020-0694-3>
46. Koji Y, Michio K, Mitsutaka T et al (2008) Correlation between chloroplast ultrastructure and chlorophyll fluorescence characteristics in the leaves of rice (*Oryza sativa L.*) grown under salinity. *Plant Prod Sci* 11(1):139–145. <https://doi.org/10.1626/pps.11.139>
47. Amario M, Villela LB, Jardim-Messeder D et al (2023) Physiological response of *Symbiodiniaceae* to thermal stress: reactive oxygen species, photosynthesis, and relative cell size. *PLoS One* 18(8):e0284717. <https://doi.org/10.1371/journal.pone.0284717>
48. Hawkins TD, Bradley BJ, Davy SK (2013) Nitric oxide mediates coral bleaching through an apoptotic-like cell death pathway: evidence from a model sea anemone-dinoflagellate symbiosis. *FASEB J* 27(12):4790–4798. <https://doi.org/10.1096/fj.13-235051>
49. Cziesielski MJ, Schmidt-Roach S, Aranda M (2019) The past, present, and future of coral heat stress studies. *Ecol Evol* 9(17):10055–10066. <https://doi.org/10.1002/ece3.5576>
50. You J, Hu H, Xiong L (2012) An ornithine δ-aminotransferase gene *OsOAT* confers drought and oxidative stress tolerance in rice. *Plant Sci* 197:59–69. <https://doi.org/10.1016/j.plantsci.2012.09.002>
51. Shaghaf Ejaz, Shah Fahad, Muhammad Akbar Anjum et al (2020). Role of osmolytes in the mechanisms of antioxidant defense of plants. In: Lichtfouse, E. (eds) Sustainable agriculture reviews 39.

Sustainable Agriculture Reviews, 39. Springer, Cham. https://doi.org/10.1007/978-3-030-38881-2_4

52. Zhi Zhou, Kaidian Zhang, Lingui Wang et al (2021) Nitrogen availability improves the physiological resilience of coral endosymbiont *Cladocopium goreaui* to high temperature. *J Phycology* 57. <https://doi.org/10.1111/jpy.13156>

53. DuRose JB, Scheuner D, Kaufman RJ et al (2009) Phosphorylation of eukaryotic translation initiation factor 2 α coordinates rRNA transcription and translation inhibition during endoplasmic reticulum stress. *Mol Cell Biol* 29(15):4295–4307. <https://doi.org/10.1128/MCB.00260-09>

54. Rosic NN, Pernice M, Dove S et al (2011) Gene expression profiles of cytosolic heat shock proteins Hsp70 and Hsp90 from symbiotic dinoflagellates in response to thermal stress: possible implications for coral bleaching. *Cell Stress Chaperones* 16(1):69–80. <https://doi.org/10.1007/s12192-010-0222-x>

55. Leggat W P, Seneca F, Wasmund K et al (2011) Differential responses of the coral host and their algal symbiont to thermal stress. *PLoS ONE*, 6. <https://doi.org/10.1371/journal.pone.0026687>

56. Cunning R, Baker AC (2020) Thermotolerant coral symbionts modulate heat stress-responsive genes in their hosts. *Mol Ecol* 29(15):2940–2950. <https://doi.org/10.1111/mec.15526>

57. Pinzón JH, Kamel B, Burge CA et al (2015) Whole transcriptome analysis reveals changes in expression of immune-related genes during and after bleaching in a reef-building coral. *Royal Soc Open Sci* 2(4):140214. <https://doi.org/10.1098/rsos.140214>

58. Zeb A, Khan Y, Yang X et al (2024) Impact of temperature stress on *Pyropia yezoensis* and its inhabitant microbiota to promote aquaculture. *Environ Adv* 16:100532. <https://doi.org/10.1016/j.envadv.2024.100532>

59. Sun Y, Jiang L, Gong S et al (2022) Changes in physiological performance and protein expression in the larvae of the coral *Pocillopora damicornis* and their symbionts in response to elevated temperature and acidification. *Sci Total Environ* 807:151251. <https://doi.org/10.1016/j.scitotenv.2021.151251>

60. Kos-Braun IC, Jung I, Koš M et al (2017) Tor1 and CK2 kinases control a switch between alternative ribosome biogenesis pathways in a growth-dependent manner. *PLoS Biol* 15(3):e2000245. <https://doi.org/10.1371/journal.pbio.2000245>

61. Shi J, Chen Y, Xu Y et al (2017) Differential proteomic analysis by iTRAQ reveals the mechanism of *Pyropia haitanensis* responding to high temperature stress. *Sci Rep* 7:44734. <https://doi.org/10.1038/srep44734>

62. González-Pech RA, Hughes DJ, Strudwick P et al (2022) Physiological factors facilitating the persistence of *Pocillopora aliciae* and *Plesiastrea versipora* in temperate reefs of south-eastern Australia under ocean warming. *Coral Reefs* 41:1239–1253. <https://doi.org/10.1007/s00338-022-02277-0>

63. Roth M, Goericke R, Dehenn D (2012) Cold induces acute stress but heat is ultimately more deleterious for the reef-building coral *Acropora yongei*. *Sci Rep* 2:240. <https://doi.org/10.1038/srep00240>

64. Krause GH, Somersalo S (1989) Fluorescence as a tool in photosynthesis research: application in studies of photoinhibition, cold acclimation and freezing stress [and Discussion]. *Philos Trans R Soc B Biol Sci* 323(1216):281–293. <https://doi.org/10.1098/rstb.1989.0010>

65. Rezayan M, Niknam V, Ebrahimzadeh H (2019) Oxidative damage and antioxidative system in algae. *Toxicol Rep* 6:1309–1313. <https://doi.org/10.1016/j.toxrep.2019.10.001>

66. Allocati N, Masulli M, Di Ilio C et al (2018) Glutathione transferases: substrates, inhibitors and pro-drugs in cancer and neurodegenerative diseases. *Oncogenesis* 7:8. <https://doi.org/10.1038/s41389-017-0025-3>

67. Gulevsky AK, Relina LI (2013) Molecular and genetic aspects of protein cold denaturation. *Cryo Letters* 34(1):62–82

68. Adjirackor N A, K E Harvey, and S C (2020) Harvey, Eukaryotic response to hypothermia in relation to integrated stress responses. *Cell Stress Chaperones*. 25(6): p. 833–846 <https://doi.org/10.1007/s12192-020-01135-8>

69. Chung-An Lu, Huang C-K, Huang W-S et al (2020) DEAD-box RNA helicase 42 plays a critical role in pre-mRNA splicing under cold stress. *Plant Physiol* 182(1):255–271. <https://doi.org/10.1104/pp.19.00832>

70. Wagner E, Lykke-Andersen J (2002) mRNA surveillance: the perfect persist. *J Cell Sci* 115(Pt 15):3033–3038. <https://doi.org/10.1242/jcs.115.15.3033>

71. Kose S, Imamoto N (1840) Nucleocytoplasmic transport under stress conditions and its role in HSP70 chaperone systems. *Biochimica et Biophysica Acta (BBA) - General Subjects* 1840(9):2953–2960. <https://doi.org/10.1016/j.bbagen.2014.04.022>

72. Biedka S, Wu S, LaPeruta AJ et al (2017) Insights into remodeling events during eukaryotic large ribosomal subunit assembly provided by high resolution cryo-EM structures. *RNA Biol* 14(10):1296–1313. <https://doi.org/10.1080/15476286.2017.1297914>

73. Gorman AM, Healy SJM, Jäger R et al (2012) Stress management at the ER: regulators of ER stress-induced apoptosis. *Pharmacol Ther* 134(3):306–316. <https://doi.org/10.1016/j.pharmthera.2012.02.003>

74. Perinur Bozaykut, Nesrin Kartal Ozer, Betul Karademir et al (2014) Regulation of protein turnover by heat shock proteins. *Free Radical Biol Med* 77. <https://doi.org/10.1016/j.freeradbiomed.2014.08.012>

75. Ha JS, Lee JW, Seo SH et al (2019) Optimized cryopreservation of *Ettlia* sp. using short cold acclimation and controlled freezing procedure. *J Appl Phycol* 31:2277–2287. <https://doi.org/10.1007/s10811-019-1743-z>

76. Duprey Y, Bhagooli R, Daniels C (2017) Gene expression biomarkers of heat stress in scleractinian corals: promises and limitations. *Comp Biochem Physiol Part C: Toxicol Pharmacol* 191:63–77. <https://doi.org/10.1016/j.cbpc.2016.08.007>

77. Tuckett CA, Thomas W (2018) High latitude corals tolerate severe cold spell. *Front Marine ence* 5:14. <https://doi.org/10.3389/fmars.2018.00014>

Publisher's Note Springer Nature remains neutral with regard to jurisdictional claims in published maps and institutional affiliations.